

# Helium trapping and clustering in ThO<sub>2</sub>

Kuganathan, N., Ghosh, P. S., Arya, A. & Grimes, R. W.

Published PDF deposited in Coventry University's Repository

## Original citation:

Kuganathan, N, Ghosh, PS, Arya, A & Grimes, RW 2018, 'Helium trapping and clustering in ThO<sub>2</sub>' Journal of Nuclear Materials, vol. 507, pp. 288-296.

<https://dx.doi.org/10.1016/j.jnucmat.2018.05.006>

DOI 10.1016/j.jnucmat.2018.05.006

ISSN 0022-3115

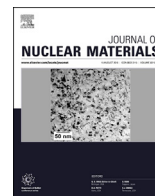
Publisher: Elsevier

## Creative Commons Attribution License (CC BY)

This article is available under the terms of the Creative Commons Attribution License (CC BY). You may copy and distribute the article, create extracts, abstracts and new works from the article, alter and revise the article, text or data mine the article and otherwise reuse the article commercially (including reuse and/or resale of the article) without permission from Elsevier. You must give appropriate credit to the original work, together with a link to the formal publication through the relevant DOI and a link to the Creative Commons user license above. You must indicate if any changes are made but not in any way that suggests the licensor endorses you or your use of the work.

Permission is not required for this type of reuse.

Copyright © and Moral Rights are retained by the author(s) and/ or other copyright owners. A copy can be downloaded for personal non-commercial research or study, without prior permission or charge. This item cannot be reproduced or quoted extensively from without first obtaining permission in writing from the copyright holder(s). The content must not be changed in any way or sold commercially in any format or medium without the formal permission of the copyright holders.



## Helium trapping and clustering in ThO<sub>2</sub>

N. Kuganathan<sup>a, \*</sup>, P.S. Ghosh<sup>b</sup>, A. Arya<sup>b</sup>, R.W. Grimes<sup>a</sup>

<sup>a</sup> Department of Materials, Imperial College London, London, SW7 2AZ, UK

<sup>b</sup> Material Science Division, Bhabha Atomic Research Centre, Trombay, Mumbai 400 085, India



### HIGHLIGHTS

- Density functional theory calculations together with dispersion corrections (DFT + D) have been employed to systematically study the stability of single He atoms at pre-existing neutral and charged point defects, smaller and larger defect clusters.
- Incorporation of He at octahedral interstitial site is energetically unfavourable compared to gas phase He. Oxygen and thorium vacancies offer more favourable He incorporation sites.
- The energy penalty to incorporate a He into the charged tetra vacancy (CTV) is almost zero. Multiple neutral tri vacancy (NTV) clusters accommodate multiple He atoms with no energy penalty.
- A relationship was generated that describes the incorporation energy of the xth He atom,  $E_x(n, m)$ , into a cluster consisting of n thorium vacancies and m oxygen vacancies.

### ARTICLE INFO

#### Article history:

Received 6 February 2018

Received in revised form

20 April 2018

Accepted 2 May 2018

Available online 5 May 2018

#### Keywords:

DFT

Helium

Incorporation energy

Thoria

Nuclear materials

### ABSTRACT

Helium, generated in nuclear fuel, accommodates into bubbles and degrades mechanical stability. Atomic scale simulations were used to study the interaction of He atoms with point defects and defect clusters. The incorporation of a single He atom was unfavourable at an octahedral interstitial site by 0.92 eV compared to the gas phase reference state, by 0.68 eV at an oxygen vacancy and by 0.32 eV at a Th vacancy. The decreasing values reflect the greater space available for the inert He atom. Defect clusters consisting of multiple oxygen and Th vacancies provide more space. Thus, incorporation at a di-vacancy required 0.31 eV, at a neutral tri-vacancy (NTV) 0.25 eV and at a tetra-vacancy 0.01 eV. Clusters formed of two and three NTVs exhibited no energy penalty for the incorporation of multiple He atoms. Relative to incorporation at an interstitial site, clusters offer space for multiple He and may therefore be effective traps to form proto-bubbles. A relationship was generated that describes the incorporation energy of the xth He atom,  $E_x(n, m)$ , into a cluster consisting of n thorium vacancies and m oxygen vacancies. Solution energies for He, where equilibrium with the solution site is taken into account, were also determined.

© 2018 The Authors. Published by Elsevier B.V. This is an open access article under the CC BY license (<http://creativecommons.org/licenses/by/4.0/>).

### 1. Introduction

In nuclear reactors, He atoms ( $\alpha$ -particles) are produced under normal operating conditions, as well as during storage of spent fuel [1]. He is produced through  $\alpha$ -decay of actinides, ternary fissions and  $^{17}\text{O}(n, \alpha)^{14}\text{C}$  reactions [2]. During normal reactor operation, intragranular He is formed which readily diffuses into the fuel-clad gap due to its low solubility in the fuel matrix and fast transport mechanism [3,4]. The long term storage of spent fuel also results in the formation of a considerable amount of He due to large

concentrations of  $\alpha$ -particle emitters ( $^{238}\text{Pu}$ ,  $^{242}\text{Cm}$ ,  $^{244}\text{Cm}$ ,  $^{241}\text{Am}$ , etc) [5]. Over time He accumulates as bubbles at grain boundaries causing severe degradation of grain cohesion and mechanical stability. It is therefore important to evaluate the energetics of He incorporation and migration in the oxide lattice. The importance of He is well recognized in  $\text{UO}_2$  and  $\text{PuO}_2$  and there have been extensive experimental and theoretical studies to evaluate its behaviour [1,3–12]. Jegadeesan et al. [13] have very recently observed aggregation and ordering in the octahedral interstitial sites in thoria.

In recent years, mixed oxide (MOX) fuels containing  $\text{ThO}_2$  are gaining attention for several reasons: (a) the natural abundance of Th and depletion of U resources (b) that Th fuels produce fewer transuranics and (c)  $\text{ThO}_2$  MOX fuels can be used to manage Pu

\* Corresponding author.

E-mail address: [n.kuganathan@imperial.ac.uk](mailto:n.kuganathan@imperial.ac.uk) (N. Kuganathan).

proliferation. Nevertheless, it can be foreseen that ThO<sub>2</sub>-based nuclear fuels [e.g. (Th,U)O<sub>2</sub>, (Th,Pu)O<sub>2</sub>] would also experience generation and diffusion of He gas during and after reactor operation, though to a lesser degree than UO<sub>2</sub> and PuO<sub>2</sub> [14].

Lu et al. [15] employed density functional theory (DFT) simulations to predict defect formation energies of neutral and charged defects in ThO<sub>2</sub>. They predicted He incorporation energies into: a neutral O vacancy, a neutral Th vacancy and an octahedral interstitial site. They concluded that the most favourable incorporation site for He is at the Th vacancy. In their calculations they did not consider He incorporation into charged defect sites. Shao et al. [16,17] recently used DFT to study the stability of single He atoms at neutral and charged point defects and smaller defect clusters in ThO<sub>2</sub>. They also considered multiple He but at interstitials and smaller neutral defect clusters only.

Here, we have used plane wave based DFT calculations to systematically study the stability of single He atoms at pre-existing neutral and charged point defects, smaller and larger defect clusters. We also report solution energies (i.e. taking account of site formation) for the most favourable trap sites. This study also identified the number of He atoms that could be accommodated at a point defect or cluster before further incorporation exceeds the interstitial incorporation limit. This allows us to comment on the mechanism for the bubble formation.

## 2. Simulation methods

The calculations were carried out using the spin-polarized mode of DFT as implemented in the VASP package [18,19]. The exchange-correlation term was modelled using the generalized gradient approximation (GGA) parameterized by Perdew, Burke, and Ernzerhof (PBE) [20]. The standard projected augmented wave (PAW) potentials [21] and a plane-wave basis set with a cut off value of 500 eV were employed. The valence electronic configurations treated for Th, He and O were 6s<sup>2</sup> 6p<sup>6</sup> 6d<sup>2</sup> 7s<sup>2</sup>, 1s<sup>2</sup> and 2s<sup>2</sup> 2p<sup>4</sup> respectively. In order to describe the behaviour of the localized Th *f* states we included the orbital-dependent, Coulomb potential (Hubbard U) and the exchange parameter J within the DFT + U calculations, as formulated by Liechtenstein et al. [22]. We applied the values of U = 4.5 eV and J = 0.5 eV to the localized *f* states of Th. Charged defects interact with their periodic images. In a previous study [23] we described the methodology as implemented by Makov et al. [24] to compensate for image charges in the defect formation calculation. In the DFT + U calculations, metastable states may be obtained for system containing 5-*f* orbital occupations. In UO<sub>2</sub>, metastable energy states have been observed as each U has an electronic configuration of 5f<sup>2</sup>. Unlike UO<sub>2</sub>, in ThO<sub>2</sub>, metastable states will not be observed as 5f orbital is vacant.

A 2 × 2 × 2 supercell containing 96 atoms was used for the defect calculations. This supercell has a lattice constant of 11.29 Å. In our previous work [23], we have used this supercell to calculate the formation energies of point defects with different charge states (from neutral to full charge). The results were in good agreement with the calculations that used a 2 × 2 × 2 supercell [15] and a 3 × 3 × 3 supercell [25]. For defect clusters consisting of multiple NTV units, a 3 × 3 × 3 supercell containing 324 atoms was used. Structural optimizations were performed using a conjugate gradient algorithm [26] and the forces on the atoms were obtained from the Hellmann-Feynman theorem including Pulay corrections. In all optimized structures, forces on the atoms were smaller than 0.001 eV/Å and the stress tensor was less than 0.002 GPa.

Due to He being chemically inert, the inclusion of van der Waals (vdW) interactions is particularly important for the calculation of incorporation energies. In this work, dispersion has been included by using the pair-wise force field as implemented by Grimme et al.

[27] in the VASP package. Energies are reported with and without the van der Waals (vdW) correction.

The quality of the pseudopotentials and basis sets were previously assessed by reproducing the experimentally observed equilibrium lattice constants, bulk modulus, cohesive energies and band gaps of bulk Th and ThO<sub>2</sub> [23]. Further, series of isolated point defect (vacancy and interstitial) energies, were calculated and combined to determine the formation energies for Frenkel and Schottky disorder and the results were validated against other theoretical studies.

## 3. Incorporation of He at interstitial, point defect and cluster sites

### 3.1. Helium atoms at interstitial site

Three interstitial positions (a face-centered position, an octahedral position and an edge center position between two oxygen atoms) were considered for the incorporation of a single He atom. Each configuration was relaxed but irrespective of starting configuration, the He atom shifted to the octahedral interstitial position. This suggests that the only possible trap site for the incorporation of a single He atom in defect-free ThO<sub>2</sub> is the octahedral interstitial position. The incorporation energy of a He gas atom in the octahedral interstitial site was calculated using the following equation:

$$E[He_i] = E[He_iTh_nO_{2n}] - E[Th_nO_{2n}] - E[He] \quad (1)$$

Where  $E[He_iTh_nO_{2n}]$  is the energy of a He atom incorporated into a ThO<sub>2</sub> supercell,  $E[Th_nO_{2n}]$  is the total energy of the defect-free ThO<sub>2</sub> supercell and  $E[He]$  is the energy of a single He gas atom. Using this approach, the calculated incorporation energy is 0.92 eV showing that incorporation is thermodynamically unfavourable (note: since the energy to create an interstitial site is zero, in this case incorporation and solution energies are identical). The Bader charge on the He atom is 0.06 *e*, which implies that the He atom retains its electronic configuration. Before and after the incorporation of the He atom, the magnetic moment of the supercell is zero. Lu et al. [15] and Shao et al. [16] considered a He atom in an octahedral position in ThO<sub>2</sub> and their reported incorporation energies were 0.77 eV and 0.75 eV respectively agreeing with the current value. In a previous study [23], the incorporation energies of Kr (6.96 eV) and Xe (10.19 eV) were calculated at octahedral positions. These values are much higher than the incorporation energy of He due to their larger size (He < Kr < Xe).

Next, two He atoms were incorporated in defect-free ThO<sub>2</sub>. Three possible initial configurations were considered. For the first two configurations, He atoms were placed at two different octahedral interstitial sites such that they were oriented (a) in a [110] direction and (b) in a [100] direction. In the third configuration two He atoms were placed at edge center positions between two O atoms. Upon relaxation, in the first two configurations He atoms retained their positions but in the third configuration He atoms moved towards the interstitial position forming a dumbbell configuration with a He-He distance of 1.48 Å. The relaxed structures are shown in Fig. 1.

The incorporation energies for the second He atom to occupy either an adjacent octahedral interstitial site or to form dumbbell configuration were 0.72 eV and 2.49 eV respectively. The results show that, the accommodation of a second He at an adjacent interstitial site in ThO<sub>2</sub> is still unfavourable though slightly less unfavourable than if the two He atoms are isolated (by 0.20 eV). The total energy of the third configuration (Fig. 1c) is 1.78 eV higher than that of the first two configurations (Fig. 1a and b). Thus, a second He will greatly prefer to occupy a separate, perhaps an

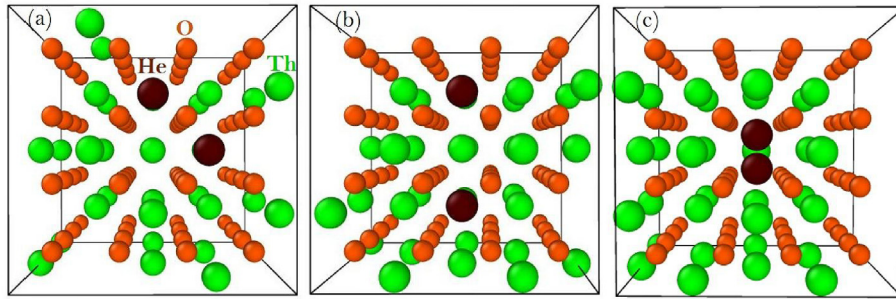


**Fig. 1.** Relaxed configurations of two He atoms in ThO<sub>2</sub>. In (a) and (b) the two He atoms are in two different octahedral interstitial sites; (c) both He atoms occupy a single octahedral site forming a dumbbell configuration.

adjacent, interstitial site. Lattice volume expansion was calculated in all three cases and compared with a 96-atom ThO<sub>2</sub> supercell. There is a 1.66 Å<sup>3</sup> increase in volume for the first two configurations and a 4.81 Å<sup>3</sup> increase for the dumbbell configuration.

Next the maximum number of He atoms that can be accommodated at an octahedral interstitial position without generating defects was identified. Up to six He atoms were placed at edge center positions and the atoms relaxed. Fig. 2 shows the relaxed structures of the most stable clusters containing 3, 4 and 5 He atoms. Three and four He atoms formed trigonal planar and square planar structures respectively without displacing the lattice ions surrounding the clusters. If the number of He atoms is greater than four, there is a substantial distortion of the lattice with the displacement of O ions. Other cluster structures in the form of trigonal pyramid, trigonal bipyramid, square pyramid and octahedral at an interstitial position were also considered. Relaxed structures are shown in the electronic supplementary information (ESI). Thus, we systematically calculated the relative energies of isolated He interstitials, interstitial plus small clusters, mixtures of small clusters and single clusters. In all cases alternative configurations in which single He atoms occupy distinct interstitial sites were found to be lower in energy.

### 3.2. Incorporation of He gas atoms at single point defects

Point defects were also considered as they can provide more space for the accommodation of He atoms. O and Th vacancy defect sites with different charge states, including full ionic charges, were modelled (vacancy clusters were also considered but are reported in a subsequent section). The absolute incorporation energy of a He atom at a defect site, for example He at a pre-existing O vacancy site, is given by,

$$E[\text{He}(V_0)] = E[\text{HeTh}_n\text{O}_{2n-1}] - E[\text{Th}_n\text{O}_{2n-1}] - E[\text{He}] \quad (2)$$

Where  $E[\text{HeTh}_n\text{O}_{2n-1}]$  is the total energy of a ThO<sub>2</sub> supercell containing a He atom at an O vacancy and  $E[\text{Th}_n\text{O}_{2n-1}]$  is the total energy of the ThO<sub>2</sub> cell containing an unoccupied O vacancy.

Absolute incorporation energies were also used to investigate if the occupation of a given defect (i.e. a Th or O vacancy) by a gas atom will alter its most stable (preferred) charged state (as described in earlier work on Kr and Xe incorporation [23]). This is achieved by reconstituting the incorporation energy relationship by adding the energy to change the charge of the vacancy from its most stable (i.e. in Kröger-Vink notation [28]  $V_{\text{Th}}^m$  or  $V_0^{\bullet\bullet}$ ) to the alternate charge (as described by equation (3)). Here, for example, He at an O vacancy with +1 charge was calculated using the following equation:

$$E_{\text{FC}}[\text{He}(V_0^{\bullet})] = E[\text{He}(V_0^{\bullet\bullet})] + \{E_f[V_0^{\bullet}] - E_f[V_0^{\bullet\bullet}]\} \quad (3)$$

where  $E_{\text{FC}}[\text{He}(V_0^{\bullet})]$  is the relative incorporation energy of He with respect to the O vacancy with +2 charge (i.e. the most favourable unoccupied charge state for an oxygen vacancy),  $E[\text{He}(V_0^{\bullet\bullet})]$  is the absolute incorporation energy of He and  $E_f[V_0^{\bullet}]$  and  $E_f[V_0^{\bullet\bullet}]$  are the formation energies of O vacancies with +1 and +2 charges respectively.

#### 3.2.1. Oxygen vacancy

Three different charge states (0, +1 and +2) were considered. The results show that the highest charged vacancy ( $V_0^{\bullet\bullet}$ ) provides the lowest incorporation energy (see Table 1). This is due in part to the induced dipole attraction between the positive charge in the cell and the electrons in the complete outer shell of He. Nevertheless, the process remains clearly endothermic. Bader charge analysis indicates that the He atom retains its electronic

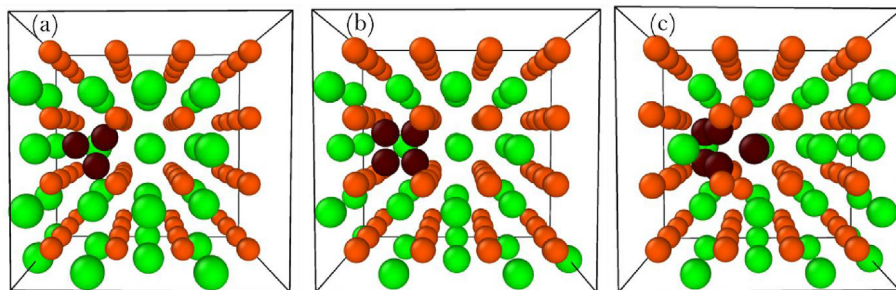


**Fig. 2.** Relaxed configurations of (a) trigonal planar (b) square planar and (c) distorted cluster configuration (with the formation of an O vacancy and an O interstitial at an interstitial) in ThO<sub>2</sub>.

**Table 1**

He incorporation energies at oxygen vacancies with 0, +1 and +2 charges, incorporation energies relative to most stable  $V_O^{\bullet\bullet}$  vacancy and net magnetic moments of the supercell. Incorporation energies calculated without dispersion corrections are shown in parentheses.

Properties	$V_O^{\times}$	$V_O^{\bullet}$	$V_O^{\bullet\bullet}$
Incorporation energy in site as charged (eV)	2.90 (3.02)	2.09 (2.19)	0.68 (0.78)
Relative incorporation energy, with respect to fully charged defect (eV)	4.33 (4.45)	2.35 (2.45)	0.68 (0.78)
Magnetic moment ( $\mu_B$ )	1.98	1.00	0.00

configuration in all charge states because of its stable closed shell configuration. Incorporation energies relative to that in the  $V_O^{\bullet\bullet}$  defect show that the He atom prefers to occupy the  $V_O^{\bullet\bullet}$  site (i.e.  $He_O^{\bullet\bullet}$ ), the same as found for Xe and Kr previously [23]. The incorporation energy of a He atom at a  $V_O^{\times}$  was calculated to be 2.48 eV by Lu et al. [15] in their GGA calculations agreeing reasonably well with the current value.

The Bader charge and the magnetic moment before and after the incorporation were also calculated. In all three cases essentially zero charge (0.06  $e$ ) is predicted. Magnetic moments of the supercell containing O vacancy defects with +2, +1 and 0 charge states but no He are 0.00, 1.00 and 0.00 respectively. Table 1 reports that the O vacancy with a full charge has no magnetic moment before and after incorporation, thus incorporation does not change magnetization. For the O vacancy with +1 charge (i.e.  $V_O^{\bullet}$ ) He incorporation also has no effect on the magnetism. However, for the neutral vacancy, incorporation of He induces a magnetic moment of 1.97  $\mu_B$ . This implies the pair of electrons that occupy the neutral site have become unpaired due to He accommodation. However, since this incorporation process is of such high energy, the effect will not be observed.

Finally, the incorporation energy was calculated for an interstitial He atom at an octahedral interstitial site but adjacent to the most favourable O vacancy (i.e.  $V_O^{\bullet\bullet}$ ). The calculated value is 0.94 eV, that is, essentially the same as at an isolated interstitial site. The presence of the vacancy therefore infers no advantage on interstitial incorporation and thus interstitial He will not be attracted to the region around a  $V_O^{\bullet\bullet}$ . A similar small increase of 0.10 eV was calculated for He in  $UO_2$  [3].

Since incorporation at a  $V_O^{\bullet\bullet}$  site offers a lower incorporation energy, two He atoms were placed in a supercell containing an O vacancy defect. Six different ways of arranging the two He atoms were considered (as shown in Fig. S3 of the ESI). The lowest energy configuration was found to be when one of the He atoms occupied the O vacancy ( $He_O^{\bullet\bullet}$ ) and the second occupied an octahedral interstitial site. However, if the He atom occupied an interstitial site close to the  $He_O^{\bullet\bullet}$  or one further away (but in the relaxed supercell) the difference in the total energy was negligible. Further, while one of the initial configurations consisted of two He atoms placed at the  $V_O^{\bullet\bullet}$ , the relaxation simulation resulted in one of the He atoms being shifted to the adjacent octahedral interstitial site showing that there is no barrier to this lowest energy configuration. Similarly two dumbbell configurations were modelled consisting of two He atoms occupying an octahedral interstitial site with an adjacent

(unoccupied) O vacancy. In the first configuration, the O vacancy was closer to the dumbbell and in the second configuration the O vacancy was away from it. The dumbbell configuration away from the O vacancy retained its configuration but the incorporation energy was less favourable. With the first configuration, one He atom relaxed to occupy the oxygen vacancy and the other He atom occupied its adjacent interstitial site again resulting in the lowest energy configuration.

The incorporation energy calculated for a second He atom to occupy an interstitial site adjacent to a  $He_O^{\bullet\bullet}$  was 0.75 eV. This is 0.17 eV less than the incorporation energy calculated for a single He occupying an interstitial site in a defect-free  $ThO_2$  supercell and 0.19 eV less than incorporating He into an interstitial site adjacent to an unoccupied O vacancy with +2 charge. Thus, once the  $V_O^{\bullet\bullet}$  defect incorporates a He (i.e.  $He_O^{\bullet\bullet}$ ) other  $He_i$  defects are attracted to the surrounding region.

### 3.2.2. Thorium vacancy

Next, incorporation was considered at a Th vacancy with different charge states. The calculations indicate that for all charge states, the incorporation energies are very similar and smaller than the equivalent values for incorporation at  $V_O^{\bullet\bullet}$  and interstitial sites (see Table 2). This is due to the relative size of the He atom compared to the larger space provided by the Th vacancy. This is further supported by the essentially zero Bader charges on He atoms at vacancy sites. The incorporation energy calculated at the neutral vacancy is 0.34 eV, close to the value of 0.21 eV calculated by Lu et al. [15]. Shao et al. [16] also calculate a values of 0.21 eV at the neutral vacancy but energies fall slightly as the vacancy charge increases, as reported in Table 2, whereas our current values remain almost constant. This difference is in part due to different methodologies used to correct for periodic charged defects. The current study used the methodology implemented by Leslie and Gillan [29], which employs the internally consistent dielectric constant, whilst Shao et al. [14] used a potential alignment correction based on macroscopic average techniques [30,31]. Also Shao et al. [16] did not include a dispersion correction and employed only a GGA functional not GGA + U. Nevertheless, both sets of values indicate incorporation proceeds with lower energy compared to that in oxygen vacancies or at an interstitial site.

The magnetic moments calculated for He free but thorium vacancy containing supercells with 0, −1, −2, −3, and −4 charges are 3.79, 2.87, 1.87, 0.87 and 0.00 respectively. After the incorporation of a He atom, corresponding magnetic moments are 3.65, 2.80, 1.82,

**Table 2**

Absolute incorporation energies of a single He atom into the four charge states of a Th vacancy; incorporation energies into the four charge states but relative to the most stable  $V_{Th}^{\bullet\bullet}$  defect. Absolute incorporation energies due to Shao et al. [16] are also reported for comparison. Incorporation energies calculated without dispersion corrections are shown in parentheses.

Properties	$V_{Th}^{\times}$	$V_{Th}^{\bullet}$	$V_{Th}^{\bullet\bullet}$	$V_{Th}^{\bullet\bullet\bullet}$	$V_{Th}^{\bullet\bullet\bullet\bullet}$
Incorporation energy (eV) (this study)	0.34 (0.44)	0.34 (0.42)	0.32 (0.42)	0.34 (0.42)	0.32 (0.43)
Relative incorporation energy, with respect to $V_{Th}^{\bullet\bullet}$ (eV)	8.66 (8.76)	6.18 (6.26)	4.03 (4.13)	1.84 (1.92)	0.32 (0.43)
Incorporation energy (eV) (Shao et al. [16])	0.21	0.18	0.17	0.14	0.07

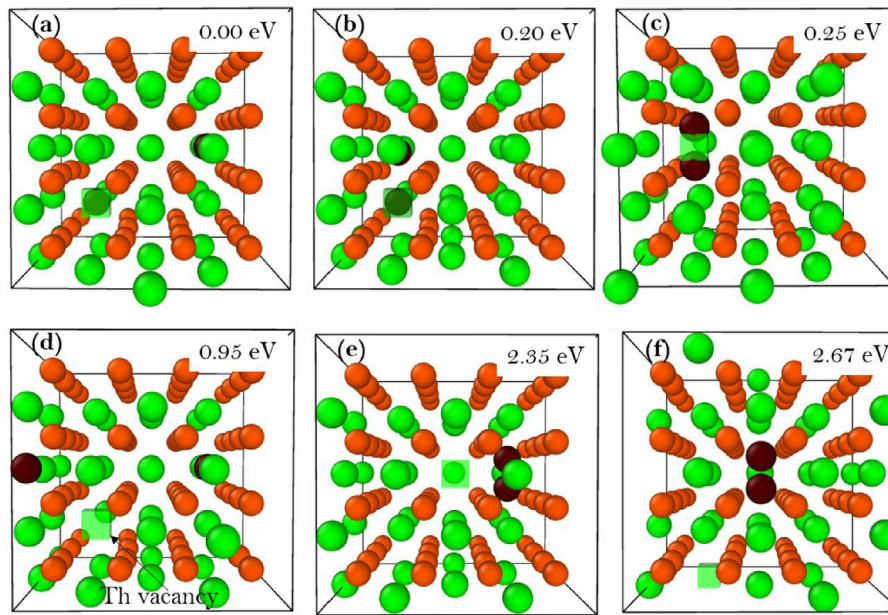


**Fig. 3.** Six different relaxed configurations together with relative energies of two He atoms occupying a supercell containing a  $V_{Th}'''$  defect.

0.81 and 0.00 respectively, showing essentially no change.

The relative incorporation energy (see Table 2) was then calculated by adding the energy to change the vacancy from its most stable  $V_{Th}'''$  to the alternative charge. Thus,  $V_{Th}'''$  is clearly the favoured incorporation site for He as observed previously for Xe and Kr incorporation [23].

Next, incorporation was considered of a He atom to an interstitial site adjacent to an unoccupied  $V_{Th}'''$  and compared to the incorporation energy calculated in the absence of the Th vacancy. The incorporation energy is 0.81 eV. Thus, the presence of a thorium vacancy reduces the incorporation energy by 0.11 eV compared to an isolated interstitial but is 0.49 eV higher than when the He occupies a vacant Th site. This is similar to that observed in the classical simulation of He in  $UO_2$  [3]. Thus, unlike the  $V_O^{\bullet\bullet}$  defect,  $V_{Th}'''$  develops an effective radius within which He at interstitial sites are energetically drawn to the  $V_{Th}'''$  defect.

In order to consider two He atoms in a supercell with a  $V_{Th}'''$  defect, six initial configurations were considered. The first configuration (Fig. 3a) had the first He at a Th vacancy,  $He_{Th}'''$ , and the second He atom at an interstitial site away from the Th vacancy. In the second configuration (Fig. 3b), the second He atom was placed in an interstitial site adjacent to the Th vacancy. In the third configuration (Fig. 3c), two He atoms were placed in a Th vacancy. In the fourth configuration (Fig. 3d), both He atoms were away from the Th vacancy. In the fifth and sixth configurations (Fig. 3e and f) a dumbbell configuration was formed closer to and away from the unoccupied  $V_{Th}'''$  defect respectively. The first configuration (3a) exhibited the lowest incorporation energy. However, the second and the third configurations were only slightly higher in energy, by 0.20 and 0.25 eV respectively. Given that there is only 0.05 eV difference in energy between configurations 2 and 3, the formation of a (non-bonded) dimer is possible if a He interstitial atom moves adjacent to a  $He_{Th}'''$  defect. The incorporation energies for the second He atom in the first, second and third configurations, assuming that the first He atom occupies the Th vacancy, are 0.63 eV, 0.83 eV and 0.88 eV respectively. These values are slightly smaller than the energy for an isolated He at an interstitial site, again indicating a higher concentration of He interstitial adjacent to a  $He_{Th}'''$ .

### 3.3. Incorporation of He gas atoms at defect clusters

#### 3.3.1. Di-vacancy cluster

Next incorporation was considered at a di-vacancy cluster (DV), which is formed by removing a Th vacancy and its nearest neighbour O vacancy. There are three charge states (0,  $-1$  and  $-2$ ) possible for this cluster (termed  $V_{ThO}^X$ ,  $V_{ThO}$  and  $V_{ThO}''$ ). In our previous study [23] it was shown that the formation of  $V_{ThO}''$ , reflecting the association of  $V_O^{\bullet\bullet}$  and  $V_{Th}'''$ , is the lowest energy cluster. Table 3 shows the incorporation energy, relative incorporation energy (to  $V_{ThO}''$ ) for a single He, and magnetic moments of the supercell for the three DV clusters. In all cases the Bader charges of He were zero, as was the case for all He in clusters. Similarly the magnetic moments of the cells with He were unaltered compared to values in the absence of He.

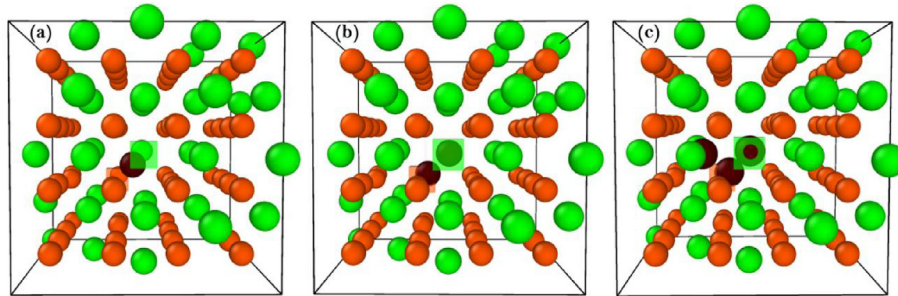
The absolute incorporation energies were very close for all three defect cluster charges and very similar to values for incorporation into thorium vacancies. However, once the relative incorporation energies were calculated with respect to  $V_{ThO}''$ , then it is the fully charged  $V_{ThO}''$  defect cluster which exhibits the lowest relative incorporation energy.

Next we considered up to 3 He atoms occupying the  $V_{ThO}''$  cluster; the relaxed structures are shown in Fig. 4. A single He atom occupies a site between the Th vacancy and the O vacancy (see Fig. 4a). For two He atoms, one of the He atoms neatly occupies the Th vacancy with the other slightly displaced from the O vacancy towards the He atom at the Th vacancy; the He-He distance is 1.99 Å. The incorporation energy calculated for the second He atom (assuming that the first He atom occupies the Th vacancy) is 0.19 eV, slightly less than the first incorporation energy. When a third He atom is added to a DV cluster with two He atoms, the relaxed structure (see Fig. 4c) shows the third He atom at the adjacent interstitial site, but displaced towards the other two He atoms. The final configuration can be considered as a cluster close to an isosceles trimer with the He-He distances of 2.02 Å, 2.04 Å and 2.48 Å. The energy to incorporate the third He atom to the (non-bonded) configuration is 0.58 eV. This is 0.34 eV less than the incorporation energy for He at an isolated interstitial site in defect

**Table 3**

Absolute incorporation energies, incorporation energies relative to  $V_{ThO}''$  and magnetic moments of the clusters. Incorporation energies calculated without dispersion corrections are shown in parentheses.

Properties	$V_{ThO}^X$	$V_{ThO}'$	$V_{ThO}''$
Incorporation energy (eV)	0.28 (0.36)	0.29 (0.38)	0.31 (0.40)
Relative incorporation energy with respect to fully charged defect (eV)	9.45 (9.53)	3.98 (4.07)	0.31 (0.40)
Magnetic moment ( $\mu_B$ )	1.87	0.94	0.00

**Fig. 4.** Relaxed structures of (a) one, (b) two and (c) three He atoms in a  $V_{ThO}''$  defect cluster.

free  $ThO_2$ . A similar situation was observed for the 4th, 5th, 6th, 7th and 8th He atoms with consistent incorporation energies from 0.58 eV to 0.60 eV, accommodated at adjacent interstitial sites. Only with the 9th He did the incorporation energy increase to 0.99 eV, similar to that for He at an isolated interstitial site. Thus, the cluster reduces the incorporation energies at the majority of adjacent interstitial sites resulting in an energetic advantage for interstitial He to be trapped close to the cluster. Thus, the  $V_{ThO}''$  cluster will trap two He in the cluster and attract 6 additional adjacent interstitial He.

### 3.3.2. Neutral tri-vacancy (NTV) clusters

Next neutral tri-vacancies (NTV) clusters were considered, formed by incorporating a second near neighbour oxygen vacancy to a DV cluster. There are three possible NTV clusters namely NTV1, NTV2 and NTV3. In the NTV1 cluster the two oxygen vacancies are oriented closest together. In the NTV2 and NTV3 clusters the two oxygen vacancies are oriented intermediate and furthest away respectively (but still near neighbour to the  $V_{Th}'''$ ) (see Ref. [22]). Table 4 reports incorporation energies and incorporation energies relative to the most stable NTV2 cluster. Magnetic moments of all cells incorporating NTV clusters were zero, with and without He incorporation (this remains the same when multiple He accommodation is considered).

The lowest incorporation energy for a single He atom is in the NTV1 cluster, as also observed by Shao et al. [16] and in our previous study for Xe and Kr [23] and Cl, Br and I [32]. This is due to the He atom being able to access the space provided by all three component defects [see Fig. S4 (a)]. The incorporation energies calculated for NTV2 and NTV3 clusters are slightly higher and the same. This is because the He, occupies the Th vacancy shifted towards only one of the O vacancies [see Fig. S4 (f) and (k)]. Relative incorporation energies (i.e. with respect to the most stable NTV2

geometry) favour the NTV2 cluster. This is because differences in absolute incorporation energies are smaller than differences between the formation energies of the three clusters. In the previous study [23] it was shown that for Xe and Kr, both incorporation energies and relative incorporation energies favoured the NTV1 geometry. This was a consequence of the much lower incorporation energy found in a NTV1 defect due to the much larger sizes of Xe and Kr.

Next occupation of up to 10 He atoms was considered in the three NTVs. Fig. S4 shows the relaxed configurations of  $He_n$  ( $n = 1$  to 5). He atoms were systematically added to each NTV cluster and the incorporation energies to add each additional He atom determined (see Table 5). The incorporation of 2nd or 3rd He atoms into any of the 3 clusters incurs an energy penalty of between 0.12 eV and 0.26 eV per He. Furthermore, the sum of incorporation energies for the first 3 He atoms into any of the clusters is only  $\sim 0.65$  eV (the same as for a single He in a  $V_{Th}''$  vacancy) and much less than the incorporation of a He at an isolated interstitial site. Even beyond 3 He, the incorporation of a 4th or a 5th He is only  $\sim 0.5$  eV/He. Clearly the NTV is a strong sink for interstitial He. Turning to the issue of

**Table 5**

Energies to incorporate successive He atoms into the three NTV defect clusters.

	Incorporation energy (eV)		
	NTV1	NTV2	NTV3
He:HeNTV	0.28	0.12	0.14
He:2HeNTV	0.17	0.26	0.27
He:3HeNTV	0.47	0.54	0.54
He:4HeNTV	0.33	0.56	0.56
He:5HeNTV	0.55	0.53	0.54
He:6HeNTV	0.56	0.54	0.54
He:7HeNTV	0.55	0.53	0.55
He:8HeNTV	0.60	0.82	0.56
He:9HeNTV	0.96	0.77	0.94

**Table 4**

Absolute incorporation energies and incorporation energies relative to the NTV2 cluster. Incorporation energies calculated without dispersion corrections are shown in parentheses.

Properties	He:NTV1	He:NTV2	He:NTV3
Incorporation energy (eV)	0.15 (0.22)	0.25 (0.34)	0.25 (0.34)
Relative incorporation energy with respect to the most stable NTV2 geometry (eV)	0.77 (0.85)	0.25 (0.34)	0.45 (0.54)

relative incorporation energy, while NTV1 does provide lower incorporation energies, even for the 4th and 5th He atoms, the overall energy of the NTV2 cluster remains lower so that even with 5 He atoms, NTV2 remains the most favourable lowest energy configuration - it may at this point even be described as a proto-bubble.

Analysing the position of He with respect to the vacant site, the first three He atoms occupied positions commensurate with the three lattice sites. The subsequent 6 atoms occupied adjacent octahedral interstitial sites around NTV1 and NTV3 clusters. The 10th He also occupies an octahedral site but further away from the cluster. For the 4th to 8th He atoms occupied adjacent octahedral interstitial sites but the 9th and 10th He atoms preferred to occupy octahedral interstitial further away. It seems the number of adjacent interstitial He with lower energy is cluster dependent but 5 or 6 should be expected for small clusters.

Comparing to equivalent values calculated by Shao et al. [17], energies to incorporate the 2nd and 3rd He are relatively similar for all three NTVs. However, Shao et al. [17] predict incorporation energies in excess of 1.5 eV for 4th He and even high for subsequent He. We presume this indicates these He atoms are somehow restricted to the vicinity of the NTV cluster, since we find no barrier to the movement of He to adjacent interstitial sites. While significantly smaller incorporation energies were also observed in the case of single Xe and Kr in NTVs compared to  $V_{O}^{**}$  and  $V_{Th}^{***}$  traps, the incorporation energies for a second Xe or Kr were prohibitively high [23].

### 3.3.3. Charged tetra-vacancy (CTV) cluster

The next cluster considered was the charged tetra-vacancy (CTV), consisting of two thorium vacancies and two oxygen vacancies with overall charge  $-4$ . Occupation by up to 10 He atoms was considered. The incorporation energy for the first He atom was 0.01 eV (see Table 6) lower than incorporation of the first He into NTV defects. This atom occupied one of the vacant Th sites. Incorporation energies for additional He atoms were also low, up to four He atoms, with these occupying the second thorium vacancy and then two vacant oxygen sites of the cluster. Addition of the 5th to 10th He atoms demands slightly more energy (see Table 6) but with values similar to the 4th to 9th He additions to the NTV clusters, still well below values for incorporation at interstitial sites. These atoms occupied adjacent interstitials sites. The 11th He demanded a higher energy, closer to that for an isolated interstitial and occupies a site slightly further away from the cluster.

### 3.3.4. Bi neutral tri-vacancies (BNTV)

In order to offer more space to accommodate He atoms, leading to the formation of a larger bubble, two NTV1 defects were associated. There are many different possible configurations. Here, as an example, we consider a BNTV with two adjacent NTV1s forming a

larger more spherical like space (see Ref [21] for details). Nine He atoms were incorporated one by one with incorporation energies reported in Table 7. The first two He atoms incorporate with essentially zero energy penalty. These atoms occupied the two vacant Th sites. Incorporation of the next two He atoms also proceeds with very low energy (i.e. less than 0.2 eV). These atoms occupy vacant oxygen sites, as did the next two He atoms although their energies were higher, similar to the subsequent atom even though this 7th He occupies an interstitial site. Values increase from 8th onwards similar to energies for the 4th He in NTV clusters and 5th He in the CTV cluster and occupy adjacent interstitial positions. It was not sensible to proceed to even greater He numbers as by this point the cluster occupies much of the computational repeat cell. Thus, we can only say the current results are consistent with at least four He atoms occupying adjacent interstitial sites with energies below 0.70 eV.

### 3.3.5. Tri neutral tri-vacancies (TNTV)

In order to increase the cavity size further, a third NTV1 was introduced to create an example tri-NTV cluster (TNTV). Up to 11 He atoms were introduced into the defect. The incorporation energies reported in Table 8 shows that the first two values are negative. The energy penalty for the addition of 3rd, 4th and 5th He atoms are then very small though positive. However, the cavity size is now such that cavities must be interacting to the extent that the incorporation energies should only be considered as indicative. Nevertheless, it is clear that the larger cluster will accommodate more He with low incorporation energy.

## 3.4. Mechanism for the bubble formation

In this section, we propose a classification for the incorporation energetics of successive He atoms to defects and small cavities (or clusters), which could be associated with the initial stage of bubble formation. In Table 9 three regimes are defined (these could be

**Table 6**  
Energies to incorporate successive He atoms into the CTV defect cluster.

	Incorporation energy (eV)
He:CTV	0.01
He:HeCTV	0.21
He:2HeCTV	0.13
He:3HeCTV	0.15
He:4HeCTV	0.42
He:5HeCTV	0.45
He:6HeCTV	0.59
He:7HeCTV	0.61
He:8HeCTV	0.58
He:9HeCTV	0.62
He:10HeCTV	0.76

**Table 7**  
Energies to incorporate successive He atoms into a BNTV defect cluster.

	Incorporation energy (eV)
He:BNTV	-0.03
He:HeBNTV	-0.03
He:2HeBNTV	+0.11
He:3HeBNTV	+0.10
He:4HeBNTV	+0.27
He:5HeBNTV	+0.35
He:6HeBNTV	+0.31
He:7HeBNTV	+0.56
He:8HeBNTV	+0.56
He:9HeBNTV	+0.58
He:10HeBNTV	+0.59

**Table 8**  
Energies to incorporate successive He atoms into a TNTV defect cluster.

	Incorporation energy (eV)
He:TNTV	-0.10
He:HeTNTV	-0.05
He:2HeTNTV	+0.07
He:3HeTNTV	+0.08
He:4HeTNTV	+0.03
He:5HeTNTV	+0.22
He:6HeTNTV	+0.15
He:7HeTNTV	+0.32
He:8HeTNTV	+0.38
He:9HeTNTV	+0.14
He:10HeTNTV	+0.33

**Table 9**

Number of He atoms accommodated in the three different regimes based on the incorporation energies  $E_x(n,m)$  successive He addition into a cluster consisting n thorium vacancies and m oxygen vacancies.

Defect clusters	Number of point defects		Incorporation energy (eV) Regimes		
			Regime I Substitutional ( $E_x < 0.05$ eV)	Regime II Substitutional ( $0.05 < E_x < 0.40$ eV)	Regime III Interstitial ( $0.40 < E_x < 0.68$ eV)
	n	m			
DV	1	1	0 (n-1)	2 (m)	6
NTV2	1	2	0 (n-1)	3 (m+1)	5
CTV	2	2	1 (n-1)	3 (m+1)	6
BNTV	2	4	2 (n)	5 (m+1)	>4
TNTV	3	6	2 (n-1)	-7 (m+1)	>2

described as regions though regimes I and II spacially overlap). Regime I is where the incorporation energy is less than  $\sim 0.05$  eV (see Table 9). These He atoms substitute at thorium vacancies but are surrounded also by oxygen vacancies. They are the first He atoms to occupy the cavity. The first cluster to offer such a low incorporation energy is the CTV. Presumably this reflects the cavity volume available compared to the He  $1s^2$  electron density. On the basis of the current work it seems that the number of He atoms that fall within this category, per n thorium vacancy components of the cavity, is (n-1).

Regime II corresponds to He atoms that are accommodated at the oxygen vacancies of the cavity and perhaps a thorium vacancy if the incorporation energy at the thorium vacancy was in excess of 0.05 eV. In all cases incorporation energies are below 0.40 eV (i.e. far below the interstitial incorporation energy). All vacancies that are components of the cavity offer incorporation energies of this magnitude or less. So, if m is the number of oxygen vacancy components of the cavity, m or perhaps (m+1) He atoms are accommodated within this regime. Considering specific examples, the NTV2 cluster accommodates 1 He atom in regime I and 2 atoms in regime II (see Table 9). The CTV cluster accommodates 2 He atoms in regime I and 2 atoms in regime II.

In regime III, the incorporation energy of He atoms is between 0.40 and 0.68 eV and the He atoms occupy adjacent interstitial sites. Calculated incorporation energies in this region are lower than at the oxygen vacancy (i.e. 0.68 eV) and much lower than at the isolated interstitial (i.e. than 0.92 eV). This is due to the distortion and symmetry breaking of octahedral sites (see Fig. 4c) adjacent to the

cluster, which means that He atoms can shift from their perfect interstitial positions lowering their energy. For the clusters considered here, there are a clear six interstitial sites that satisfy this constraint. Presumably as the cluster size increases the number will increase to reflect the greater surface area (S) of the cluster. Thus, we can describe the number as  $6 + S$ .

In regime IV, the incorporation energy is greater than 0.68 eV. In this region, He is accommodated at essentially isolated interstitial positions.

It is now possible to express an approximate averaged relationship between the incorporation energy,  $E_x(n,m)$ , of the xth He atom and the number of point defects in the cluster. The expression is depicted in Fig. 5 as an S-shaped curve. Of course, for an actual cluster the specific geometry of the cluster will dictate small deviations from the S-shaped curve energies.

### 3.5. Solution energies

Bubbles are not equilibrium defects with respect to gas phase He. They form because they offer lower energy sites than the local state of He (e.g. at an interstitial site) or in the defect by which the He might be transported (e.g. at an oxygen vacancy). It is therefore useful to consider the equilibrium solution of He in  $\text{ThO}_2$  by calculating solution energies. These are established by combining relative incorporation energies with the formation energies of the equilibrium solution sites. The methodology and formation energies of equilibrium solution sites have been reported previously in detail [23] and allows us to consider and compare solution into

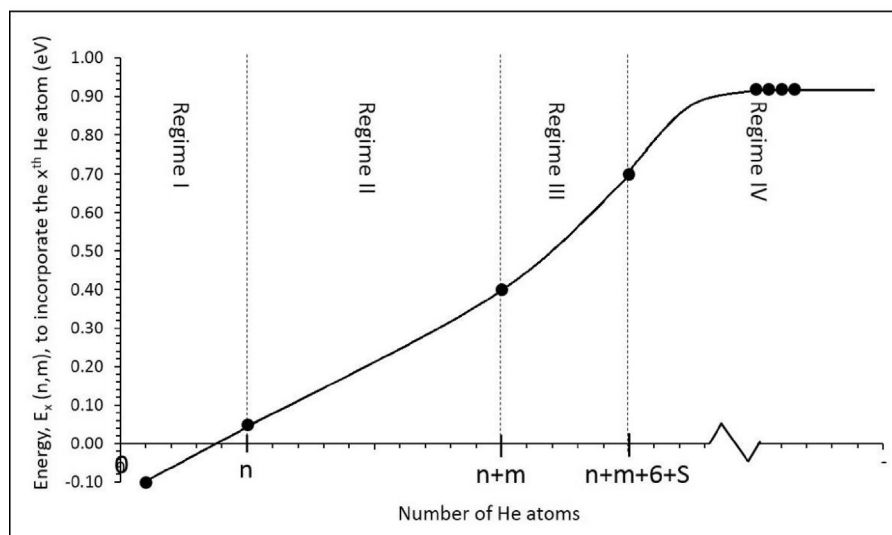


**Fig. 5.** The energy to incorporate the xth He atom,  $E_x$ , in a cluster consisting of n Th vacancies and m oxygen vacancies. Three energy regimes are identified, which corresponds to how He atoms are accommodated.

**Table 10**  
Solution energies of a single He atom in ThO<sub>2</sub> and in ThO<sub>2-x</sub>.

Int	Solution Energies (eV) in ThO <sub>2</sub>				CTV
	$V_{\text{O}}^{**}$	$V_{\text{Th}}^{**}$	$V_{\text{ThO}}^{**}$	NTV2	
<b>0.92</b>	2.99	4.64	5.51	6.02	8.60
Solution Energies (eV) in ThO <sub>2-x</sub>					
0.92	<b>0.68</b>	9.26	7.82	6.02	13.22

stoichiometric ThO<sub>2</sub> and sub-stoichiometric ThO<sub>2-x</sub>. Solution energies take into account that He concentrations may be higher than the trap (solution) site concentrations.

The solution energies (Table 10) predict the most stable (equilibrium) solution sites for He, in ThO<sub>2</sub> and ThO<sub>2-x</sub> are interstitial and  $V_{\text{O}}^{**}$  respectively, as expected. These positive values indicate that the equilibrium concentration of (inert) He is very low. The difference between ThO<sub>2-x</sub> and ThO<sub>2</sub> may be significant influencing the transport mechanism, which will impact on the bubble growth rate.

#### 4. Conclusions

Atomic scale simulations based on DFT have been employed to study the interaction of He atoms with point defects and clusters of point defects. Incorporation of He at octahedral interstitial sites is energetically unfavourable compared to gas phase He, but is where much He will initially reside once the concentration of He is greater than the equilibrium concentration of point defects, since He is generated within the lattice. Oxygen and thorium vacancies offer more favourable He incorporation sites but still demand 0.68 eV and 0.32 eV respectively compared to the gas phase. The oxygen vacancy is particularly important in sub-stoichiometric ThO<sub>2-x</sub>. Further reduction in the incorporation energies is observed with defect clusters due to the increased space available to accommodate He. The energy penalty to incorporate a He into the CTV is almost zero. Multiple NTV clusters accommodate multiple He atoms with no energy penalty. Nevertheless, eventually as more He is added to a cluster the incorporation energy of each successive atom increases but four regimes can be identified, corresponding to how the He is accommodated. In Regime I, He is accommodated at a Th vacancy with incorporation energy 0.05 eV/He or less. When He is incorporated in Regime II the energy penalty falls between 0.05 eV/He and 0.40 eV/He. These atoms fill up the vacant oxygen sites. Around the cluster are adjacent interstitial sites. These are filled in Regime III, which will accommodate He with energy between 0.40 eV/He to that required by an isolated oxygen vacancy (i.e. 0.68 eV/He). Beyond this, Regime IV is where He is accommodated at effectively isolated interstitial sites further away from the cluster. These energy partitions are used to generate a cluster average relationship for the incorporation energy,  $E_x(n, m)$  of the  $x$ th He atom into a cluster consisting of  $n$  thorium vacancies and  $m$  oxygen vacancies.

#### Acknowledgement

We thank the EPSRC for funding as part of the INDO-UK project (grant code EP/K00817X/1). Computational facilities and support

were provided by High Performance Computing Centre at Imperial College London.

#### Appendix A. Supplementary data

Supplementary data related to this article can be found at <https://doi.org/10.1016/j.jnucmat.2018.05.006>.

#### References

- [1] F. Garrido, L. Nowicki, G. Sattonnay, T. Sauvage, L. Thomé, Nucl. Instrum. Meth. B 219–220 (2004) 196.
- [2] D. Roudil, J. Bonhoure, R. Pik, M. Cuney, C. Jégou, F. Gauthier-Lafaye, J. Nucl. Mater. 378 (2008) 70.
- [3] R.W. Grimes, R.H. Miller, C.R.A. Catlow, J. Nucl. Mater. 172 (1990) 123.
- [4] X.-Y. Liu, D.A. Andersson, J. Nucl. Mater. 498 (2018) 373.
- [5] T. Wiss, J.-P. Hiernaut, D. Roudil, J.-Y. Colle, E. Mauger, Z. Talip, A. Janssen, V. Rondinella, R.J.M. Konings, H.-J. Matzke, W.J. Weber, J. Nucl. Mater. 451 (2014) 198.
- [6] C.O.T. Galvin, M.W.D. Cooper, P.C.M. Fossati, C.R. Stanek, R.W. Grimes, D.A. Andersson, J. Phys.: Condens. Mater. 28 (2016) 405002.
- [7] E. Mauger, T. Wiss, J.P. Hiernaut, K. Desai, C. Thiriet, V.V. Rondinella, J.Y. Colle, R.J.M. Konings, J. Nucl. Mater. 385 (2009) 461.
- [8] L. Dabrowski, M. Szuta, J. Alloy. Comp. 615 (2014) 598.
- [9] Y. Yun, O. Eriksson, P.M. Oppeneer, J. Nucl. Mater. 385 (2009) 510.
- [10] X. Tian, T. Gao, C. Lu, J. Shang, H. Xiao, Eur. Phys. J. B 86 (2013) 179.
- [11] D. Gryaznov, E. Heifets, E. Kotomin, Phys. Chem. Chem. Phys. 11 (2009) 7241.
- [12] X.Y. Liu, D.A. Andersson, J. Nucl. Mater. 498 (2018) 373–377.
- [13] P. Jegadeesan, S. Amirthapandian, B.K. Panigrahi, G. Kaur, D. Sanjay Kumar, P. Magudapathy, K. Ananthasivan, J. Alloy. Comp. 743 (2018) 196–202.
- [14] T.R. Govindan Kutty, J. Banerjee, Arun Kumar, Thermophysical Properties of thorium-based fuels, in: D. Das, S. Bharadwaj (Eds.), Thorium-based Nuclear Fuels. Green Energy and Technology, Springer, London, 2013.
- [15] Y. Lu, Y. Yang, P. Zhang, J. Phys.: Condens. Mater. 24 (2012) 225801.
- [16] K. Shao, H. Han, W. Zhang, H. Wang, C.-Y. Wang, Y.-L. Guo, C.-L. Ren, P. Huai, J. Nucl. Mater. 490 (2017) 181.
- [17] S. Kuan, H. Han, Z. Wei, W. Chang-Ying, G. Yong-Liang, R. Cui-Lan, H. Ping, Chin. Phys. B 26 (2017) 097101.
- [18] G. Kresse, J. Furthmüller, Phys. Rev. B 54 (1996) 11169.
- [19] G. Kresse, D. Joubert, Phys. Rev. B 59 (1999) 1758.
- [20] J.P. Perdew, K. Burke, M. Ernzerhof, Phys. Rev. Lett. 77 (1996) 3865.
- [21] P.E. Blöchl, Phys. Rev. B 50 (1994) 17953.
- [22] A.I. Liechtenstein, V.I. Anisimov, J. Zaanen, Phys. Rev. B 52 (1995). R5467.
- [23] N. Kuganathan, P.S. Ghosh, C.O.T. Galvin, A.K. Arya, B.K. Dutta, G.K. Dey, R.W. Grimes, J. Nucl. Mater. 485 (2017) 47.
- [24] G. Makov, M.C. Payne, Phys. Rev. B 51 (1995) 4014.
- [25] S.T. Murphy, M.W.D. Cooper, R.W. Grimes, Solid State Ionics 267 (2014) 80.
- [26] W.H. Press, B.P. Flannery, S.A. Teukolsky, W.T. Vetterling, Numerical Recipes: the Art of Scientific Computing, 1986, 818 pp.
- [27] S. Grimme, J. Antony, S. Ehrlich, H. Krieg, J. Chem. Phys. 132 (2010) 154104.
- [28] F.A. Kröger, H.J. Vink, Relations between the Concentrations of Imperfections in crystalline solids, in: S. Frederick, T. David (Eds.), Solid State Physics, Academic Press, 1956, p. 307.
- [29] M. Leslie, N.J. Gillan, J. Phys. C Solid State Phys. 18 (1985) 973.
- [30] A. Baldereschi, S. Baroni, R. Resta, Phys. Rev. Lett. 61 (1988) 734.
- [31] M. Pressi, N. Binggeli, A. Baldereschi, J. Phys. D Appl. Phys. 31 (1998) 1273.
- [32] N. Kuganathan, P.S. Ghosh, A.K. Arya, G.K. Dey, R.W. Grimes, J. Nucl. Mater. 495 (2017) 192.